ELSEVIER

Polymer 42 (2001) 1383–1391

polymer

www.elsevier.nl/locate/polymer

Glass transition induced by solvent desorption for statistical MMA/*n*BMA copolymers — Influence of copolymer composition

A.-C. Saby-Dubreuil[a], B. Guerrier[a,*], C. Allain[a], D. Johannsmann[b]

[a]*Laboratory FAST (Université Pierre et Marie Curie — Université Paris Sud — CNRS) Bât. 502, Campus Universitaire, 91405 Orsay, France*
[b]*Max Planck Institute for Polymer Research, Ackermannweg 10, 55128 Mainz, Germany*

Received 28 March 2000; received in revised form 4 July 2000; accepted 17 July 2000

Abstract

An experimental study of the glass transition induced by solvent desorption has been performed for a series of Methyl methacrylate (MMA)/*n*-butyl methacrylate (*n*BMA) statistical copolymer films. The glass transition temperature of the dry homopolymers, PMMA and P*n*BMA, are, respectively, about 105 and 7°C above the temperature of the experiment, so that the glass transition domain can be analyzed in detail by varying the solvent concentration and the copolymer composition. A strong coupling was found between drying dynamic and stress relaxation. In particular, the quantitative analysis of the desorption isotherms based on the Leibler–Sekimoto approach led to a bulk modulus *K* that increases as the proportion of *n*BMA increases, contrary to the behavior of dry annealed samples. © 2000 Elsevier Science Ltd. All rights reserved.

Keywords: Methyl methacrylate/*n*-butyl methacrylate copolymer films; Glass transition; Solvent desorption

1. Introduction

Copolymers are extensively used in industrial processes, because their physical properties (elasticity, permeability, glass transition temperature, solvent diffusion kinetics) can be varied within wide limits. Various theoretical and experimental studies on copolymers have extended the theoretical approaches previously developed for homopolymers. Some of these works focus on block copolymers, which exhibit specific properties due to mesophase formation. The behavior of statistical copolymers, most commonly used in industrial applications for practical reasons, are also of great interest.

This paper concerns an experimental study of solvent sorption and desorption by statistical copolymer films, which undergo a glass transition. The glass transition temperature of a polymer/solvent solution increases as the solvent concentration decreases. Consequently, as a polymer solution dries, the glass transition occurrence depends both on the temperature and on the concentration in the film. A good understanding of these phenomena is important from both the fundamental and practical points of view. For example, in the food packaging industry, polymer films have to meet severe requirements, such as very low residual solvent content, specific mechanical properties and permeability properties, all of which is in complex dependency on the overall drying and cooling kinetics, and especially on the solvent diffusion through the polymer matrix and the glass transition of the film.

In this study, we focus on the solvent-induced glass transition, for a series of copolymers. The solvent diffusion (polymer/solvent mutual diffusion coefficient) is not considered here: preliminary results have already been given [26], and more complete results will be published later. Methyl methacrylate (MMA) and *n*-butyl methacrylate (*n*BMA) are the two components of the copolymers used in our study. They were chosen because the glass transition temperature of the pure polymers are very different — $T_{g0} = 130$°C for PMMA and $T_{g0} = 32$°C for P*n*BMA — while the temperature in our sorption/desorption experiments is about 25°C. So, during solvent concentration variations, the PMMA solution clearly crosses the glass transition, while the P*n*BMA solution remains rubbery except at very low solvent concentrations. By varying the ratio of MMA and *n*BMA monomers in the copolymers, the variation of the copolymer properties between these two limits can be investigated. Let us notice that the two polymers PMMA and P*n*BMA are not miscible, so that a blend of the two components would lead to segregation phenomena, whereas copolymerization offers intermediate properties between the two homopolymers.

* Corresponding author. Fax: +33-1-69-15-80-60.
E-mail address: guerrier@fast.u-psud.fr (B. Guerrier).

PII: S0032-3861(00)00539-5

The sorption and desorption experiments were performed in a pressure controlled chamber, where the solvent pressure is slowly increased (sorption experiments) or decreased (desorption experiments) by control valves. The solvent pressure variations are slow compared to the characteristic time of solvent diffusion through the film so that we can assume that the solvent concentration is uniform at all times through the film. The film weight variation is measured using a quartz crystal microbalance.

This article is organized as follows. Section 2 gives a brief presentation of the theoretical models used to analyze the data. The sample preparation and experimental setup are described in Sections 3 and 4. Qualitative analysis and quantitative results concerning the variation of copolymer properties with composition are given in Section 5.

2. Theoretical background

At the glass transition, a dramatic change occurs in the local motion of the polymer chains that leads to large changes in several physical properties. For example, Young's modulus drops steeply by a factor of 10^3 typically between the glassy regime and the rubbery regime. More precisely, Gilbert et al. [12] distinguish four regimes of deformation for amorphous polymers, the glassy and viscous regimes at temperatures well below and well above the glass transition temperature, respectively, and the glass transition and rubbery regimes around T_{g0}. These regimes involved different deformation mechanisms which have to be described by different theoretical approaches.

Let us remind that only solvent-induced glass transition is considered here, the dry polymers being glassy at the temperature of the experiment ($T \simeq 25°C$) The glass transition temperature (T_g) of the polymer/solvent solution varies with the concentration and, for experiments performed at a constant temperature, the transition occurs when the solvent volume fraction reaches φ_{Sg} (i.e. the polymer volume fraction reaches $\varphi_{Pg} = 1 - \varphi_{Sg}$).

2.1. Rubbery domain

In the rubbery domain (when the polymer film is swollen) the classical Flory–Huggins' expression is used to get the activity versus solvent content in the film:

$$a = P_{VS}/P_{VS0} = (1 - \varphi_P) \exp(\varphi_P + \chi\varphi_P^2) \quad (1)$$

where a, the activity, is the ratio of the saturated vapor pressure of the solvent in equilibrium with the solution (P_{VS}) to the saturated vapor pressure of the pure solvent (P_{VS0}), φ_P is the polymer volume fraction and χ is the Flory–Huggins interaction parameter which characterizes the affinity between the solvent and the polymer.

In a first Flory–Huggins' theory, the interaction parameter χ was assumed to be independent of the concentration. Further developments have extended this model including a concentration dependence of the interaction parameter [25,27]. Regarding the case of copolymers, the Flory–Huggins' theory has been extended to blends of homopolymers and statistical copolymers: it has been shown that the interaction parameter of the blend deviates from a simple weighted average and depends on the interactions of the two components of the copolymer. Shiomi et al. [31] found the same effect experimentally for copolymer/solvent solutions (MMA/*n*BMA and cyclohexanone). Various other thermodynamic vapor–liquid equilibrium models for copolymers/solvent solutions have also been reported for example by Bogdanic and Fredenslund [2]. Examples of deviation from ideal behavior can be found in Gupta and Prausnitz's paper [14].

2.2. Glassy domain

When going from the molten to the glassy state, the variation of the solvent content with the activity shows a dramatic change and the sorption isotherms exhibit a pronounced downward curvature: for a given activity, the solvent content is much higher than what is predicted by the Flory–Huggins theory (see Fig. 2). Several theoretical approaches have been developed to describe solvent solubility in the glassy domain. In the dual-mode sorption model, it is interpreted in terms of sorption of penetrant into specific sites (microvoids) that exist only in the glassy state. The solubility then includes two contributions, the first corresponding to Flory–Huggins dissolution and the second to Langmuir hole-filling [1]. More recently, new approaches have been proposed that do not assume the existence of specific absorption sites: Vrentas and Vrentas [33] relate excess sorption to the change of the specific heat at the glass transition, while Lipscomb [19] and Leibler and Sekimoto [18] use the elastic properties of the glassy state to explain the excess solvent content. Lipscomb extends the Flory–Huggins' theory to materials with nonzero internal energy changes due to deformation. Sorption isotherms deduced from this theory show the typical downward curvature of the glassy domain. Leibler and Sekimoto express the osmotic pressure (and then the chemical potential) as a function of the bulk elastic modulus (the energy associated with the elastic deformation of the sample under volume variations is added to the usual term describing the exchange between penetrating molecules and the surroundings). Assuming that the bulk modulus is constant in the glassy state and that there is no change in the specific volumes, the following expression can be derived:

$$a = (1 - \varphi_P) \exp[\varphi_P + \chi\varphi_P^2 - \nu_S K/RT \ln(\varphi_P/\varphi_{Pg}(T))] \quad (2)$$

where K is the bulk modulus, ν_S the solvent molar volume, T the temperature, R the perfect gas constant and φ_{Pg} the polymer volume fraction at which glass transition takes place.

In the rubbery domain, elastic contribution is negligible and the activity is simply given by the classical Flory–Huggins expression. Let us emphasize that these thermodynamic approaches do not take into account the variations of

Table 1
Molecular characteristics, calorimetric data and thicknesses of spin-cast films

		PMMA	MMA/*n*BMA copolymers				P*n*BMA
			I	II	III	IV	
Proportion in monomer			84/16	64/36	48/52	28/72	
Triad analysis	mm (%)	1	3	5	7	10	2
	mr (%)	25	42	38	38	35	30
	rr (%)	74	55	57	55	55	68
M_n (kg/mol)		220	91	107	207	208	219
M_w/M_n		1.17	2.93	3.03	2.34	1.41	1.45
T_{g0} (°C)		131	96	75[a]	63	49	34
ΔC_{pp} (J/K/g)		0.24	0.28	0.24	0.27	0.24	0.30
Film thickness (nm)		220	410	580	440	860	860

[a] Extrapolated value.

the glass properties on the time scale of the sorption experiments. The bulk modulus deduced from our experimental data is then characteristic of the "average" polymer matrix state corresponding to the desorption experiments performed.

2.3. Glass transition

The comparison of experimental desorption isotherms with Leibler and Sekimoto's model gives an estimation of the transition concentration φ_{Pg} at the temperature of the experiment. It is interesting to relate this to the glass transition temperature of the dry polymer (T_{g0}). Dimarzio et al. [8] have developed a thermodynamic model predicting the fall in glass transition temperature due to a diluent as function of the diluent concentration, the length, and the stiffness energy of the diluent molecule. This model has been extended by Chow [7]; the glass transition temperature for a given value of φ_P is expressed as a function of the monomer molecular weight, the diluent concentration, and the transition isobaric heat capacity increment of the polymer:

$$\ln(T_g/T_{g0}) = \beta[(1-\theta)\ln(1-\theta) + \theta\ln(\theta)] \quad (3)$$

where T_{g0} is the glass transition temperature of the dry polymer and T_g that of the solution with polymer volume fraction φ_P. The dimensionless parameters θ and β are $\theta = \nu_M(1-\varphi_P)/z\nu_S\varphi_P$ and $\beta = zR/M_M\Delta C_{PP}$, where ν_M and ν_S are the monomer and solvent molecular volumes, z the lattice coordination number (taken as 2), R the perfect gas constant, M_M the monomer molecular weight and ΔC_{PP} the excess isobaric specific heat of transition for the polymer. This model is appropriate when the solvent molecule and monomer sizes do not differ too much and can thus be applied to the systems under study.

Another expression has been proposed by Kelley and Bueche [16], in which the glass transition temperature of the solution is expressed as a function of the polymer volume fraction, the solvent thermal expansion coefficient ($\alpha_S \sim 10^{-3}\,K^{-1}$), and the solvent glass temperature (T_{gS}) [22]:

$$T_g = [c\varphi_P T_{g0} + \alpha_S(1-\varphi_P)T_{gS}]/[c\varphi_P + \alpha_S(1-\varphi_P)] \quad (4)$$

where $c = 4.8\times10^{-4}\,K^{-1}$.

3. Materials and sample preparation

3.1. Materials

The polymer samples used in this study were kindly prepared by Thomas Wagner (Max Planck Institute for Polymer Research, Mainz, Germany). The homopolymer PMMA, poly(methyl methacrylate), was prepared by anionic polymerization in tetrahydrofuran (THF) at −80°C using diphenylbutyllithium as initiator. The homopolymer P*n*BMA, poly(*n*-butyl methacrylate), was prepared by radical polymerization at 60°C using azobis-isobutyronitril (AIBN) as initiator. The statistical methyl methacrylate/*n*-butyl methacrylate (MMA/*n*BMA) copolymers were prepared by radical polymerization in bulk at 130°C with AIBN as initiator. The resulting polymers were fractionated from a THF solution using petrolether as precipitant.

Copolymer compositions and tacticities were measured by ^{1}H NMR and ^{13}C NMR in $CDCl_3$ on 300- and 75-MHz Brucker AC-300 spectrometers. The relative concentrations of comonomers in copolymers were determined by comparing the intensities of the $-OCH_2-$ and $-OCH_3$ proton resonances, on the ^{1}H NMR spectra [5]. The ratios of isotactic (mm) to heterotactic (mr, rm) to syndiotactic (rr) triads were obtained from the quaternary carbon signal, on the ^{13}C NMR spectra [13]. Molecular weights and polydispersities were determined by GPC, relative to PMMA standard, using a Waters apparatus. The glass transition temperatures T_{g0} ("midpoint" temperatures) and the specific heat variation at the glass transition ΔC_{pp} were investigated by means of a Mettler DSC-30 differential scanning calorimeter. The heating rate was 10°C/min.

Molecular characteristics and calorimetric data are summarized in Table 1. The rather high glass transition

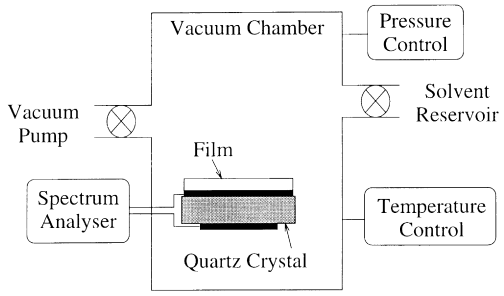

Fig. 1. Experimental setup.

temperatures of PMMA and P*n*BMA are typical values for syndiotactic-rich PMMA and P*n*BMA [10,29]. The copolymer glass transition temperatures vary monotonously with their compositions as reported by Penzel et al. [24].

Toluene (Riedel-de Haën GmbH) was used as solvent for sorption and desorption experiments.

3.2. Sample preparation

The polymer films were spin-cast directly onto the gold electrode of piezoelectric quartz crystals. Their thicknesses were chosen in the range 200 nm–1 μm (see Table 1). This constitutes a compromise between rapid diffusion, which is easily achieved for thin films, and an accurate determination of solvent weight fraction, which is more easily determined for thicker films. Moreover, large damping of the resonance occurs with films thicker than 1 μm (see next section), which has to be avoided.

The films were spin-cast from a 5 wt% (or 10 wt%) solution in toluene, with spinning rates in the range 1000–5000 rpm, the film thicknesses being adjusted by both the solution concentration and the spinning rate. When investigating the surface of the films with a profilometer (Alpha-Stepper 200 from Tencor Instruments), thickness fluctuations in the range of 5–10% of the sample thickness were found. These thickness variations do not affect our results critically.

4. Experimental

4.1. Weight determination

Quartz crystal resonators are a comparatively easy and precise tool for determining the weight of thin films [20,32]. When a thin film is cast onto one of the electrodes of a thickness-shear resonator, its acoustical resonance frequencies change due to the weight of the film. For a sufficiently thin film, the relation between weight and frequency shift (for the *n*th harmonic) is given by the Sauerbrey equation [28]:

$$\delta m = \frac{Z_q}{2f_1}\left(\frac{\delta f}{f}\right)_n = -\frac{Z_q}{2f_1}\frac{f_n - f_{n,\mathrm{ref}}}{f_{n,\mathrm{ref}}} \quad (5)$$

where δm is the film weight per unit area, f_n the frequency of the *n*th harmonic, $f_{n,\mathrm{ref}}$ the frequency of the *n*th harmonic for the unloaded quartz, f_1 the fundamental frequency, and $Z_q = 8.8 \times 10^6$ kg m^{-2} s^{-1} the acoustic impedance of AT-cut quartz. Given an accuracy of frequency determination of about 1 Hz, monolayer sensitivity is achieved.

The Sauerbrey equation is valid only for thin films whose thicknesses are much less than the wavelength of sound $[f_n\sqrt{\rho J}]^{-1}$, where ρ is the film density and J its shear compliance ($J = J' + \mathrm{i}J''$). For polymeric materials ($G \simeq 10^7 - 10^9$ Pa, $\rho \simeq 10^3$ Kg/m^3) this amounts to a thickness between 1 and 10 μm. For thicker or softer films, viscoelastic behavior has to be taken into account and the relation between weight and frequency shifts becomes [9,15]:

$$\left(\frac{\delta f}{f}\right)_n = \frac{f_n - f_{n,\mathrm{ref}}}{f_{n,\mathrm{ref}}} = -\frac{2f_1}{Z_q}\left(\delta m + \frac{4\pi^2}{3}\frac{J'\delta m^3}{\rho}f_n^2\right) \quad (6)$$

By plotting $(\delta f/f)_n$ derived from different harmonics versus the square of the frequency f_n^2, the film weight per unit area corresponds to the offset of the line. The elastic shear compliance J' can be estimated from the slope of this line. In this work, given the film thicknesses, the weights were calculated with Eq. (6), using harmonics between 27 and 60 MHz.

The measurements were performed with optically polished AT-quartz plates with a fundamental frequency of about 4 MHz. The gold electrodes are 150 nm thick and the back electrode has key hole shape to achieve energy trapping.

The data acquisition has been described elsewhere [15,3]. Briefly, we use an HP4195 impedance analyzer (Hewlett-Packard) to determine the frequency-dependent AC admittance of the quartz resonator in the vicinity of an acoustic resonance. Because of the piezo effect, the mechanical resonance is evidenced as a Lorentz curve in the conductance spectrum. Data acquisition of the center and the bandwidth of the Lorentz curve take about 5 s per harmonic, so weight determination takes about 30 s per data point.

4.2. Experimental setup

A detailed description of the experimental setup has been given elsewhere [3]. The polymer film cast onto the quartz crystal resonator is located inside a vacuum chamber connected to a solvent reservoir (in which the solvent vapor pressure is equal to the saturated vapor pressure of pure solvent, i.e. $P_{vs0} = 28.45$ Torr at $T = 25$°C for toluene) (Fig. 1). The lowest pressure reached under continuous pumping is 10^{-3} Torr. Since the experiments are undertaken at much larger pressures, this state is called "zero pressure" in the following. A needle valve connects the chamber and the vacuum pump, and the pressure is controlled in the chamber by an electronic valve connecting the chamber to the solvent reservoir. The pressure can be kept constant for several hours and pressure ramps can be applied. Two pressure gauges are used for the ranges $P > 10$ Torr and $P < 10$ Torr. The accuracy is about

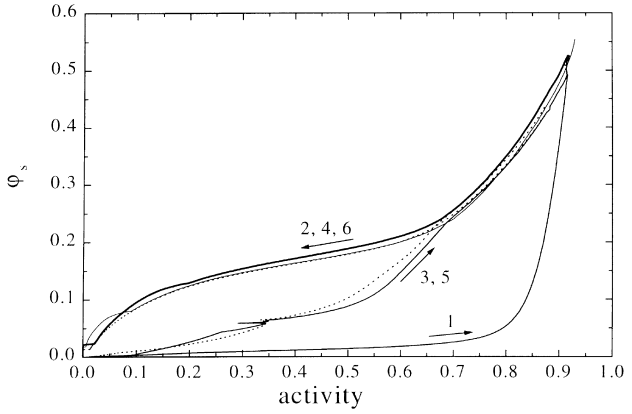

Fig. 2. Sorption and desorption curves for MMA/*n*BMA 84/16 copolymer ($m_p = m_0$) (1 = first increasing ramp, just after annealing-3,5 = other increasing ramps-2,4,6 = decreasing ramps).

0.02 Torr for $P > 10$ Torr and about 2×10^{-3} Torr for $P < 10$ Torr. Let us note that, once the film has reached equilibrium, the pressure in the chamber corresponds to the saturated vapor pressure of the solvent above the polymer film, as no inert gas is present in the chamber.

Because of temperature-frequency coupling of the quartz crystal resonator, it is necessary to have a temperature control in the chamber and in the solvent reservoir. Using a thermostat, the chamber temperature is adjusted to $T = 25 \pm 0.15$°C. The error in weight determination due to temperature fluctuations ($\Delta T \simeq 0.1$°C) was measured on blank quartz to be smaller than 5×10^{-8} kg/m^2, which corresponds to an error in solvent concentration of $\delta\omega_s \leq 0.01\%$ for a 1 μm-thick film.

The pressure effect on resonance frequencies was also investigated on blank quartz. This effect has three sources: viscous drag of the gas, pressure dependence of the elastic constants of the quartz itself, and sorption or desorption of physisorbed molecules on the quartz surface [20]. The systematic error due to pressure effects increases as pressure increases. At 25 Torr (of toluene vapor), it is about 10^{-5} kg/m^2, which corresponds to an error in solvent concentration of $\delta\omega_s \leq 0.4\%$ for a 1 μm-thick film.

4.3. Methodology for sorption/desorption experiments

Quasi-stationary experiments were carried out with slow ramps of decreasing (or increasing) pressure. The pressure variations were to be slow enough to allow diffusion equilibrium at all times. However, when the polymer is glassy, the viscoelastic relaxation equilibrium is not reached anymore.

Prior to experiment, all samples are annealed in a vacuum oven for 12 h at a temperature 50°C above their T_{g0}. Once the sample is mounted in the vacuum chamber, the vacuum is turned on for at least 10 h. The weight of the dry film is then measured. Then a series of increasing and decreasing ramps is performed without removing the film from the chamber. To drive decreasing pressure ramps, solvent vapor is first introduced in the chamber. After equilibrating the film for 90 min at about 25 Torr, the vapor is slowly removed through the needle valve connected to the vacuum pump. The pressure follows an exponential decay over a typical ramp duration of 20 h. Linear increasing pressure ramps are performed using the electronic valve connected to the solvent reservoir, with the needle valve to the vacuum pump half opened. Vacuum is applied inside the chamber for 12 h prior to the increasing ramps, typically lasting 12 h.

5. Experimental results

5.1. Definition of the variables

The pressure ramp data is presented as follows. The abscissa is the activity, i.e. the ratio between the toluene pressure measured in the chamber and the saturated vapor pressure of pure toluene at the temperature of the experiment. This saturated vapor pressure, $P_{VS0}(T)$, was obtained with Antoine's approximation.

The ordinate is the solvent volume fraction, $\varphi_S = 1 - \varphi_P$, calculated from the measured solvent weight fraction and from the specific volumes of the solvent and of the polymer, which are assumed to remain constant. The estimation of the polymer weight, m_P, is not straightforward in these experiments. Indeed, each time the pressure was decreased down to 0 Torr (end of decreasing ramps or end of large drying jumps starting at a "high" pressure), an increase in the film weight was always observed even after several hours in the vacuum. This weight increase, versus the number of dry state/swollen state cycles, first increases sharply (between the weight at 0 Torr just after annealing and the weight after the first swelling of the film) and then slows down. The total increase is quite the same for the six samples, about 3×10^{-5} kg/m^2, which corresponds to 8 wt% for the 220 nm thick PMMA film and 4wt% for the 860 nm thick PnBMA film. Two phenomena seemed to be involved. First, there is some "trapped" solvent which does not evaporate, even at 0 Torr. This was confirmed by UV investigations of PnBMA test films coated on UV quartz plates and placed in the chamber together with the films coated on the quartz microbalance. Indeed, UV spectra show the presence of a small amount of toluene in the film. A slight increase of trapped solvent is observed with film thickness but, due to the small quantities involved, no precise quantitative data could be obtained, nor any information on the location of the trapped solvent. We are thus unable to determine whether or not this solvent is thermodynamically equivalent to the solvent that swells the film when toluene pressure is increased. A second phenomenon might stem from the drift of the quartz microbalance measurement, due to some modification of the stress repartition in the film. This was deduced from experimental observations of a slow reincrease of the "apparent" weight at 0 Torr after a deswelling experiment for some of the copolymers.

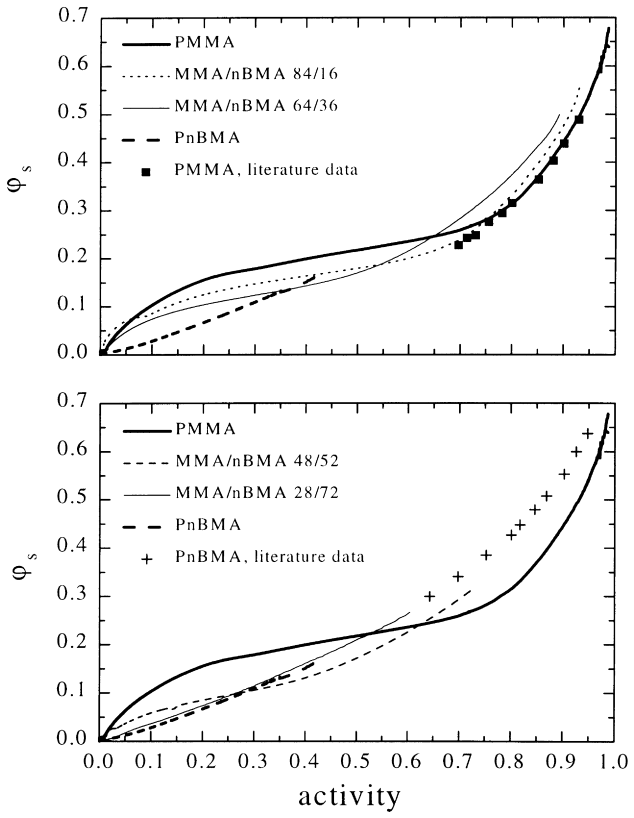

Fig. 3. Desorption curves for PMMA, P*n*BMA and MMA/*n*BMA 84/16, 64/36, 48/52 and 28/72 copolymers ($m_p = m_0$). Data from the literature for PMMA and P*n*BMA [35]. (For clarity, the curves corresponding to the copolymers are drawn in two graphs).

Given these observations, we used two estimations of the polymer weight to calculate the solvent weight fraction. In the first (noted m_{dry}) the polymer weight is always kept equal to the value measured just after annealing. In the second estimation (noted m_0), the polymer weight used corresponds to the weight obtained at the end of each decreasing ramp, after several hours in the vacuum. The real value of the polymer weight should lie between these two estimations. Let us emphasize that, despite this uncertainty, the conclusions of all the analyses are the same with these two estimations and, as shown in the following, the results are only slightly modified quantitatively.

5.2. Comparison of sorption and desorption behavior for the different copolymers

Fig. 2 shows the results obtained with successive increasing and decreasing pressure ramps for the MMA/*n*BMA 84/16 copolymer. The first increasing ramp (1) that was performed just after annealing exhibits a very large "delay" in the swelling, and strongly differs from the other swelling ramps (3 and 5). Comparing decreasing ramps 2, 4 and 6 with increasing ramps 3 and 5, we see the well-known hysteresis between the swelling and the drying behaviors. Since the pressure rate is slow compared with the characteristic diffusion time, this hysteresis is not related to diffusion effects, but originates from the incomplete stress relaxations of the polymer matrix which occur on time scales of the same order as the pressure ramps. This is why, for a given activity, the solvent content in the film depends on the polymer matrix state, and on the whole film "history". At the beginning of the first increasing ramp, the annealed film is very dense. The polymer matrix relaxes very little on the time scale of the increasing ramp and solvent sorption is inhibited, except at the very end of the ramp, close to the glassy/rubbery transition. The other increasing ramps correspond to a very different initial state of the film, since they were performed after the film had been swollen at "high" pressure and brought back to 0 Torr for a few hours. At the beginning of these increasing ramps, the film is in a pseudo-equilibrium state which differs from annealed state. Indeed, the polymer matrix is not completely relaxed and solvent sorption is easier.

The three decreasing ramps were performed after the film was swollen at "high" pressure, above the glass transition. Stresses are then relaxed, and the initial state is the same for the three experiments, so that the three curves are nearly superimposed. The solvent content for a given activity is higher than for the increasing ramps, since stress relaxations are slower than the pressure decrease rate, and the film retains the memory of its initial state. All these qualitative analyses show the importance of dynamic effects for the copolymers under study, and the complexity of relaxation regimes around the glass transition [12].

Such hysteresis is observed with PMMA and the MMA/*n*BMA 84/16, 64/36 and 48/52 copolymers. On the contrary, for MMA/*n*BMA 28/72 copolymer and P*n*BMA, the sorption and desorption curves are quite similar. Indeed, glass transition occurs for very low solvent contents, and the film is rubbery almost throughout the whole concentration domain. Stress relaxation times are short compared with the pressure rate, so that stress equilibrium is achieved all through the experiment.

The desorption curves obtained for the two homopolymers and for the four copolymers are compared in Fig. 3. The homopolymer PMMA, and the MMA/*n*BMA 84/16, 64/36 and 48/52 copolymers exhibit the characteristic kink of glass transition, but this is smoother as the proportion of *n*BMA increases. On the other hand, this feature is not discernible for MMA/*n*BMA 28/72 copolymer nor for P*n*BMA.

5.3. Variation of physicochemical parameters with the copolymer composition

Since glassy solutions are not in a true equilibrium state, the polymer matrix state depends on the experimental procedure. This is why the same experimental procedure was used with the different copolymers, and why only the desorption curves were used for quantitative comparisons with theoretical models. The film is rubbery at the beginning

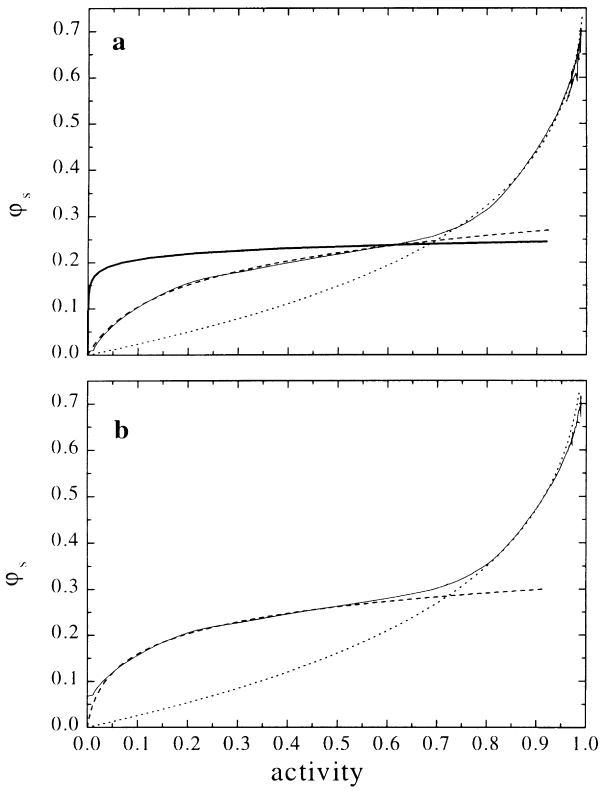

Fig. 4. Desorption curve for PMMA (solid line), Flory–Huggins' model (dot line) and Leibler–Sekimoto's model (dash line). (a) With normalization $m_p = m_0$. The estimated parameters are $\chi = 0.50$, $K = 180$ MPa and $\varphi_{Pg} = 0.75$. The heavy solid line shows Leibler–Sekimoto's model with the following parameters: $\chi = 0.50$, $K = 1$ GPa and $\varphi_{Pg} = 0.76$. (b) With normalization $m_p = m_{dry}$. The estimated parameters are $\chi = 0.42$, $K = 230$ MPa and $\varphi_{Pg} = 0.72$.

of the desorption experiment so that the initial state of the film is well defined. The successive steps of the analysis are the following: first, the interaction parameter χ is obtained by data fit in the rubbery domain. Leibler and Sekimoto's model is used to fit the desorption curves in the glassy domain, and to get the bulk modulus K and the transition concentration φ_{Pg}. This transition concentration is compared with the value obtained using Chow's and Kelley's models.

5.3.1. Flory–Huggins interaction parameter χ

The interaction parameter χ is obtained by fitting the Flory–Huggins' equation (Eq. (1)) in the rubbery domain. Let us emphasize that the experimental procedure used in this study is for purposes of studying the glass transition and is not the most accurate method for analyzing the liquid/vapor equilibrium [35,23]. For the two homopolymers, we also used experimental data from the literature [35] in the diluted domain (see Fig. 3). Practically, as can be seen on Fig. 4, a model with a constant parameter χ is suitable for an accurate data fit. The values obtained for PMMA/toluene ($\chi = 0.53 \pm 0.04$) and P*n*BMA/toluene ($\chi = 0.17 \pm 0.08$) are close to other experimental determinations: fitting Wohlfarth's data collection [35] yields $\chi = 0.17$ for P*n*BMA and $\chi = 0.51 - 0.54$ for PMMA, osmotic pressure measurements lead to $\chi = 0.45$ for PMMA ($\varphi_P \to 0$) [23] and values deduced from the second virial coefficient yield $0.37 \leq \chi \leq 0.42$ for PMMA ($\varphi_P \to 0$) [4]. The variation of χ with the copolymer composition is given in Fig. 5a. The error bars take into account the dispersion of the results obtained for the various ramps, the fit uncertainty and the uncertainty on the specific volume of the copolymers. The specific volumes of the copolymers are not known, and the specific volume of PMMA itself depends on the tacticity ($0.816 \leq V_S \leq 0.846$ cm^3/g at about 25°C) [6,30]. Despite the rather large error bars, the results show the deviation from the simple weighted average already noticed by Shiomi et al. [31] for the same copolymers in cyclohexanone, which means that the interactions between the different segments constituting the statistical copolymer affect the interaction between the copolymer and the solvent. Similar results are obtained by setting $m_P = m_{dry}$, with slightly smaller values (typically they are shifted by about 0.1).

5.3.2. Bulk modulus K and transition concentration φ_{Pg}

The bulk modulus K and the transition concentration φ_{Pg} are obtained by fitting the data with the Leibler–Sekimoto's model in the glassy domain (Eq. (2)). Due to experimental limitations, the slow decreasing pressure ramps are stopped once the pressure is less than about 1 Torr, and the valve connecting the chamber to the vacuum pump is suddenly opened wide. Then, data are not taken into account for activities less than 0.03 (i.e. $\varphi_S \leq 0.05$), since the diffusion equilibrium is no longer achieved. Leibler–Sekimoto's model depends on three unknowns, the interaction parameter χ, the transition concentration φ_{Pg} and the bulk modulus K [18]. The estimation of the relative sensitivity of the activity to these three parameters, defined as "$p_i/a\partial a/\partial p_i$" (where p_i is one of these three parameters), is straightforward. The sensitivity to χ is low compared with the sensitivity to φ_{Pg} and K, so that an error on χ does not greatly affect the estimation on the two other parameters. So the values obtained in the previous section are used for χ. The two parameters φ_{Pg} and K are estimated from the slope and the offset of the line: $y = K[\ln(\varphi_P) - \ln(\varphi_{Pg})]$, the expression for y being deduced easily from Eq. (2). The fit is made on the linear part of the y equation.

Models and experimental data are compared in Fig. 4 for PMMA. As can be seen, the agreement is very satisfactory. A same agreement is observed for the various copolymers, except for MMA/*n*BMA 28/72 copolymer and for P*n*BMA, for which glass transition occurs at a value of φ_S too small to allow reliable study of the glassy domain. The variations of K and φ_{Pg} with the copolymer composition are given in Fig. 5b and c. The error bars take into account the dispersion of the results obtained for the various ramps, the uncertainty on χ determination, and the fit uncertainty.

Let us emphasize that the bulk modulus K is an average value which corresponds to the concentration domain of the

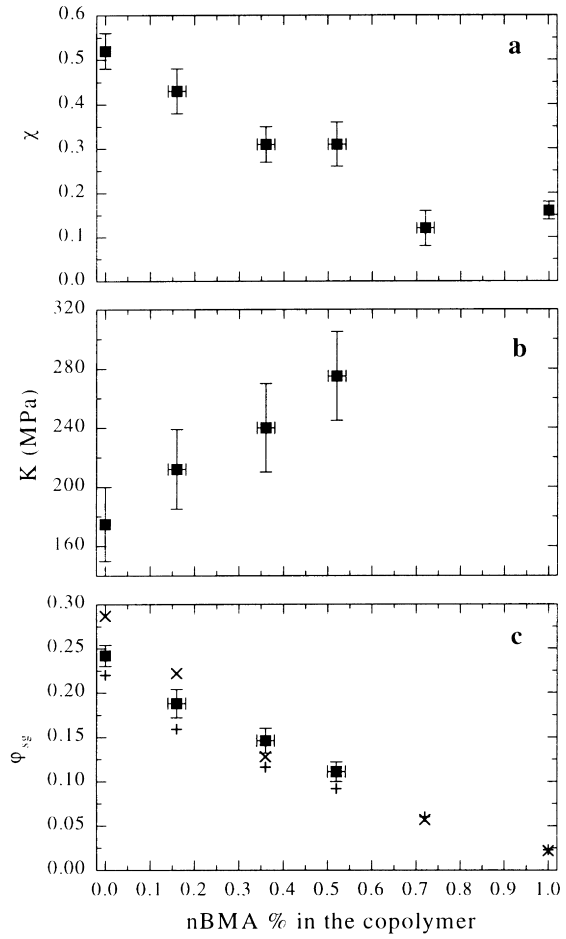

Fig. 5. Variation of the interaction parameter χ (a), the bulk modulus K (b) and the transition concentration $\varphi_{Sg} = 1 - \varphi_{Pg}(c)$ with the copolymer composition ($m_p = m_0$). Experimental data (solid square) and estimations with Chow's model (×) and Kelley's equation (+).

fit and which, above all, depends strongly on the polymer matrix state. This is very well illustrated by the variation of K versus the copolymer composition: the modulus increases as the proportion of *n*BMA in the copolymer increases, whereas the opposite variation is found in the literature for the bulk modulus measured on annealed samples. The value obtained for PMMA is more than 15 times smaller than the usual value obtained for dry annealed PMMA, which ranges between 3 and 10 GPa [17,21,11]. As an illustration Leibler and Sekimoto's model plotted with $K = 1$ Gpa (see Fig. 4a) is obviously very far from the experimental data. The bulk modulus of annealed P*n*BMA estimated from Young modulus measurements and shear modulus data from the literature [11,34] is in the range 500 MPa–2 GPa ($\nu = 0.30$–0.42). The gap between the estimated values of K and those corresponding to annealed samples decreases as the *n*BMA proportion in the copolymer increases; for PMMA and MMA-rich copolymers, the large gap is the signature of a polymer matrix structure very different from that of annealed samples.

The same procedure was repeated by setting $m_P = m_{dry}$. The conclusions are similar, i.e. the estimated bulk modulus K increases as the proportion of *n*BMA increases, though the estimated values are a little higher (they are typically shifted by about 50 MPa).

Lastly, the variation of φ_{Pg} with copolymer composition (Fig. 5c) shows good agreement with Chow's and Kelley's models (Eqs. (3) and (4)). Our results lie between the two models when using $m_P = m_0$, and are closer to the Chow's equation when using $m_P = m_{dry}$.

6. Conclusion

An experimental study of the glass transition induced by solvent desorption was performed for a series of MMA/*n*BMA copolymers. The experimental temperature (25°C) is close to the dry P*n*BMA glass transition temperature and about 100°C below the dry PMMA glass transition temperature. By varying the solvent concentration and the copolymer composition, a detailed analysis of the glass transition domain can then be performed. Complex phenomena occur in this domain, since there is a strong coupling between drying dynamic and stress relaxation, depending on the copolymer composition. Qualitative comparisons between sorption and desorption isotherms for various initial states have shown the importance of relaxation effects for the series of copolymers under study. This was confirmed by a quantitative analysis of the desorption isotherms based on the Leibler–Sekimoto's approach: the estimated bulk modulus K increases as the proportion of *n*BMA increases, contrary to the behavior of annealed samples. All this analysis was performed on pseudo-equilibrium experiments where the pressure rate is slow compared to the characteristic diffusion times. The next step of this study is to investigate the behavior of solvent diffusion coupled with glass transition as a function of solvent concentration and copolymer composition.

Acknowledgements

The authors gratefully thank Catherine Amiel for helpful advice in polymer characterization. This work was supported by PEFE (Pechiney Emballage Flexible Europe) and by a PROCOPE project (French–German Cooperation Program, no. 134).

References

[1] Berens AR. Gravimetric and volumetric study of the sorption of gases and vapors in poly(vinyl chloride) powders. Polymer Engineering and Science 1980;20(1):95–101.
[2] Bogdanic G, Fredenslund A. Prediction of vapor–liquid equilibria for mixtures with copolymers. Industrial Engineering and Chemical Research 1995;34:324–31.
[3] Bouchard C, Guerrier B, Allain C, Laschitsch A, Saby AC, Johannsmann D. Drying of glassy polymer varnishes: a quartz resonator study. Journal of Applied Polymer Science 1998;69:2235–46.

[4] Brandrup J, Immergut EH. Polymer handbook. New York: Wiley Interscience, 1989.
[5] Brar AS, Kapur GS. Sequence determination in methyl methacrylate-*n*-butyl methacrylate copolymers by ^{13}C nmr spectroscopy. Polymer Journal 1988;20(9):811–7.
[6] Bywater S, Toporowski PM. Effect of stereostructure on glass transition temperatures of poly(methyl methacrylate). Polymer 1972;13:94–96.
[7] Chow TS. Molecular interpretation of the glass transition temperature of polymer–diluent systems. Macromolecules 1980;13:362–4.
[8] Dimarzio EA, Gibbs JH. Molecular interpretation of glass temperature depression by plasticizers. Journal of Polymer Science: Part A 1963;1:1417–28.
[9] Domack A, Johannsmann D. Plastification during sorption of polymeric thin films. Journal of Applied Physics 1996;80:2599.
[10] Fernandez-Martin F, Fernandez-Pierola I. Glass transition temperature and heat capacity of heterotacticlike pmma. Journal of Polymer Science 1981;19:1353–63.
[11] Ferry JD. Viscoelastic properties of polymers. 3rd ed.. New York: Wiley, 1980.
[12] Gilbert DG, Ashby MF, Beaumont PWR. Modulus-maps for amorphous polymers. Journal of Materials Science 1986;21:3194–210.
[13] Goni I, Gurruchaga M, Valero M, Guzman GM. Determination of the tacticity of polymethacrylates obtained from graft copolymers. Polymer 1992;33(14):3089–94.
[14] Gupta RB, Prausnitz JM. Vapor–liquid equilibria of copolymer + solvent and homopolymer + solvent binaries: new experimental data and their correlation. Journal of Chemical Engineering Data 1995;40:784–91.
[15] Johannsmann D, Mathauer K, Wegner G, Knoll W. Viscoelastic properties of thin films probed with a quartz crystal resonator. Physics Review B 1992;46:7808–15.
[16] Kelley FN, Bueche F. Viscosity and glass temperature relations for polymer–diluent systems. Journal of Polymer Science, L 1961:549–56.
[17] Van Krevelen DW. Properties of polymers. Amsterdam: Elsevier, 1990.
[18] Leibler L, Sekimoto K. On the sorption of gases and liquids in glassy polymers. Macromolecules 1993;26:6937–9.
[19] Lipscomb GG. Unified thermodynamic analysis of sorption in rubbery and glassy materials. American Institute of Chemical Engineers Journal 1990;36(10):1505–16.
[20] Lu C, Czanderna AW. Applications of piezoelectric quartz crystal microbalances. Amsterdam: Elsevier, 1984.
[21] Lu H, Zhang X, Knauss WG. Uniaxial, shear, and Poisson relaxation and their conversion to bulk relaxation: studies on poly(methyl methacrylate). Polymer Composites 1997;18(2):211–22.
[22] Marcus Y. The properties of solvents. New York: Wiley, 1998.
[23] Orwoll RA. The polymer–solvent interaction parameter χ. Rubber Chemistry and Technology 1977;50:451–79.
[24] Penzel E, Rieger J, Schneider HA. The glass transition temperature of random copolymers: 1. Experimental data and the Gordon–Taylor equation. Polymer 1997;38(2):325–37.
[25] Petri HM, Wolf BA. Composition-dependent Flory–Huggins parameters: molecular weight influences at high concentrations. Macromolecular Chemistry and Physics 1995;196:2321–33.
[26] Saby-Dubreuil AC, Guerrier B, Allain C, Johannsmann D. Drying and swelling kinetics of co-*p*(mma-stat-nbma) copolymer films. In: Proc. Second European Congress of Chemical Engineering, 1999.
[27] Saeki S, Tsubokawa M, Yamaguchi T. Semiempirical determination of solution structure in polymer solutions based on the clustering theory. Macromolecules 1987;20:2930–4.
[28] Sauerbrey G. Arch. Elektrotech. Ubertragung 1964;18:617.
[29] Shetter JA. Effect of stereoregularity on the glass temperatures of a series of polyacrylates and polymethacrylates. Polymer Letters 1963;1:209–13.
[30] Shindo H, Murakami I, Yamamura H. Dielectric properties of stereoregular poly(methyl methacrylates). Journal of Polymer Science: Part A-1 1969;7:297–310.
[31] Shiomi T, Tohyama M, Endo M, Sato T, Imai K. Dependence of Flory–Huggins (parameters on the copolymer composition for solutions of poly(methyl methacrylate-ran-*n*-butyl methacrylate) in cyclohexanone. Journal of Polymer Science: Part B: Polymer Physics 1996;34:2599–606.
[32] Stockbridge CD. Vacuum microbalance techniques. New York: Plenum, 1966.
[33] Vrentas JS, Vrentas CM. Sorption in glassy polymers. Macromolecules 1991;24:2404–12.
[34] Weidisch R, Horig E, Ensslen M, Michler GH, Stamm M, Jerome R. Mechanical properties and deformation mechanisms of poly(styrene-*b*-butylmethacrylate) diblock copolymers. Polymers for Advanced Technologies 1998;9:727–33.
[35] Wohlfarth C. Vapour–liquid equilibrium data of binary polymer solutions. Amsterdam: Elsevier, 1994.